A Periodical Time-Variable Effect in OFDM Systems with Aliasing and a Sampling Frequency Offset

Ilias Trachanas and Norbert J. Fliege
Chair of Electrical Engineering
Faculty of Mathematics & Computer Science
University of Mannheim, Mannheim, Germany
Email: ilias.trachanas@ti.uni-mannheim.de

***Abstract*—Aliasing constitutes a well-known drawback of digital communication systems and causes time-invariable effects, which affect the signal to noise ratio (SNR) at the digital receiver. Orthogonal Frequency Division Multiplexing (OFDM) systems suffer besides from intercarrier interference (ICI) caused by the non-perfectly synchronized clock of the receiver. This work focuses on the study of the effects caused by the interference of these both system impediments. The infinite aliased copies of the insufficiently filtered OFDM base-band spectrum generated at the transmitter are additionally phase-distorted due to the sampling frequency offset between the receiver and the transmitter. A thorough analysis of the frequency components at every OFDM subcarrier position at the receiver shows that the received power is a periodical function of time. We explain how this effect depends on the transfer function of the utilised reconstruction and anti-aliasing low-pass filters as well as the value of the sampling frequency offset and the transmission channel. Two realistic as well as one unrealistic scenarios are investigated in order to demonstrate the theoretically studied relationships.**

***Index Terms*—Aliasing, Frequency Offset, OFDM, Synchronization, Periodical Time-Variable Effect.**

I. Introduction

Numerous advantages of the OFDM modulation technique have led to the fact that it is nowadays widely used in standards about data transfer over various mediums including telephone cables, the air, powerlines etc. However, OFDM is very sensitive to system's imperfections caused by the disability to perfectly fulfil important theoretical assumptions in practically implemented systems. Such a theoretical consideration of vital importance for every digital communication system, the discussion of which is widely found in the literature (e.g. in [1]), is the perfect low-pass filtering at the transmitter (reconstruction filtering) and at the receiver (anti-aliasing filtering).

Especially in OFDM systems a number of implementation issues concerning the computing power of modern digital signal processors or the dispose of limited bandwidth have contributed to the standardization of the policy to use the lowest possible sampling rate. By exploiting the properties of the discrete Fourier transform (DFT) in order to generate and transmit a real signal it is a common practice to add the complex-conjugated parts of the signal in the frequency domain. As a consequence of the imperfections of the reconstruction filter frequencies near to the system's Nyquist frequency are occupied, which could obstruct the parallel use of other systems that utilize these frequencies. Moreover, because of the fact that the anti-aliasing filter is also imperfect such frequency parts of the transmitted signal cause aliasing at the receiver.

The limited accuracy of the sampling frequency oscillators, which are utilized in every implemented OFDM system, counts as an additional origin for difficulties and system quality degradations. Intercarrier interference (ICI) and intersymbol interference (ISI) are the best examples of problems caused by a sampling frequency offset between transmitter and receiver [2], [3], [4]. The impact at the bit error rate is actually visible for small sampling frequency offsets. Some systems deal with the problem by measuring the offset and correcting it by means of a voltage controlled oscillator or signal interpolation techniques (e.g. interpolation of the twiddle factors [5]). Other systems use ICI correction methods [6], [7], [8], [9]. However, for reasons of cost and computing resource conservations or even simplicity and robustness other systems tolerate the sampling frequency offset by using sophisticated techniques e.g. differential phase modulation or timing offset correction methods. Moreover, the accuracy of the methods is limited and depends on the fulfilling of certain conditions, which is particularly difficult if other effects (e.g. aliasing) occur at the same time or if the channel's transfer function is still unknown.

Main objective of this work is the investigation of the effects caused by the parallel existence of aliasing and a sampling frequency offset, which is in different degrees the fact in every implemented OFDM system. In many systems yet the effect is particularly noticeable at the beginning of the link establishment during the channel measurement. While considering a number of different effects caused by the previously mentioned system's imperfections in section II we analyse the OFDM signal in different interesting positions of the communication path. Section III begins with a thorough discussion of the effects caused by aliasing and a sampling frequency offset alone. At the end of the part of the section that analyses aliasing an exact formula for the power of the signal per

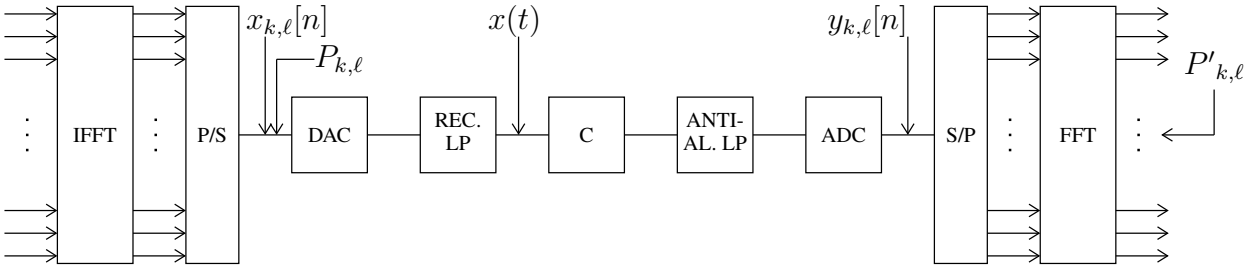

Fig. 1. A typical OFDM system

subcarrier and symbol at the output of the receiver's fast Fourier transform (FFT) is provided. As next a discussion of the effects that dominate in case of the interaction of aliasing and a sampling frequency offset as well as the analysis of the periodical time-variable received power effect caused by this interaction follows. The results of the previous paragraphs are used in section IV to demonstrate the effect in three different scenarios and show how it can be approximately eliminated and the work is closed by the conclusions.

II. The OFDM system

A typical OFDM system is shown in Fig. 1. At the transmitter the information bits are separated into packets and appropriately used as input of a modulator that calculates $\frac{M}{2}-1$ complex values, the Fourier coefficients. These values determine the amplitude $\alpha_{k,\ell}$ and the initial phase $\phi_{k,\ell}$ in the k-th OFDM symbol of $\frac{M}{2}-1$ modulated subcarriers (hereafter also called "useful" subcarriers), where ℓ denotes the subcarrier index ($1 \ll \ell \ll \frac{M}{2}-1$). Note that the subcarrier with zero index is not used because it produces zero frequency signal parts, which cannot be practically used. In order to produce a real signal at the output of the transmitter a well-known property of the FFT is utilised according to which the output of the inverse FFT (IFFT) is real only when the description of the basis-band output signal in the frequency domain (the input of the IFFT) is complex-conjugated symmetrical. For that reason the rest of the $\frac{M}{2}-1$ subcarriers (hereafter also called "useless" subcarriers as they can carry no extra information) are modulated with the same amplitude and the opposite phase of their correspondent "useful" subcarrier (subcarrier index symmetrical to $\frac{M}{2}$). Due to the fact that the signal is discrete described the hypothetical spectrum of the digital transmitted signal is composed of infinite copies of the "useful" and the "useless" subcarriers, that are moved by multiples of 2π to other frequency areas, which is graphically illustrated in Fig. 2. After the IFFT with length M the discrete time domain signal of subcarrier ℓ reads:

$$x_{k,\ell}[n] = \alpha_{k,\ell} \cdot \left(\frac{1}{2}\mathrm{e}^{\,j(\Omega_\ell n+\phi_{k,\ell})} + \frac{1}{2}\mathrm{e}^{\,-j(\Omega_\ell n+\phi_{k,\ell})}\right) \cdot \mathrm{rect}_{\,M}[n-(M-1)/2]\,,$$

where $\Omega_\ell = 2\pi\frac{\ell}{M}$ denotes the angular frequency normalised to the sampling frequency f_s and

$$\mathrm{rect}_{\,M}[n] = \begin{cases} 1\,, & |n| \le \frac{M-1}{2} \\ 0\,, & \text{otherwise} \end{cases}$$

denotes a discrete rectangular sequence. The transmitted power per symbol is then given by:

$$P_{k,\ell} = \frac{\alpha_{k,\ell}^2}{M}\sum_{n=0}^{M-1}\cos^2(\Omega_\ell n+\phi_{k,\ell}) = \frac{\alpha_{k,\ell}^2}{2} \qquad (1)$$

In order to depict the fact that before the reconstruction filter the OFDM signal contains infinite, periodically copied "useful" and "useless" subcarriers we assume that the transmitter always sends the same information bits at all subcarriers and every subcarrier is loaded with the same power. Considering the fact that the discrete Fourier transform of a discrete rectangular sequence is a Dirichlet function the frequency domain signal reads:

$$X(\Omega) = \alpha_{k,\ell}\pi\sum_{i=-\infty}^{+\infty}\mathrm{e}^{\,j\phi_{k,\ell}}\cdot\mathrm{di}\,(\Omega-\Omega_\ell-2\pi i) + \alpha_{k,\ell}\pi\sum_{i=-\infty}^{+\infty}\mathrm{e}^{\,-j\phi_{k,\ell}}\cdot\mathrm{di}\,(\Omega+\Omega_\ell-2\pi i)$$

After the FFT and a parallel to serial converter the data are given to the DAC. As already mentioned the DAC and ADC are normally of type "sample and hold" and will be hereafter handled as filters with the following transfer function (ideally exactly the same f_s is utilized at the transmitter and the receiver):

$$H_{da}(\Omega) = H_{ad}(\Omega) = \mathrm{si}\,(\Omega T_s/2)\cdot\mathrm{e}^{\,-j\Omega T_s/2} \qquad (2)$$

The si- shape of H_{da} is caused by the fact that every sample is held until the next comes, which means that the sample values are multiplied with a rectangular function ($\mathrm{rect}\,(\frac{t-T_s/2}{T_s/2})$), the Fourier transform of which is a si function.

The output of the DAC is connected to the reconstruction filter. This is an analog low-pass filter, which attenuates the "useless" subcarriers and the continuously periodical copies of them and those of the "useful" subcarriers. Depending on the form and grade of the realised reconstruction filter the amplitudes at the infinite frequency positions of the transmitted signal are decreasing with frequency to almost but not exactly

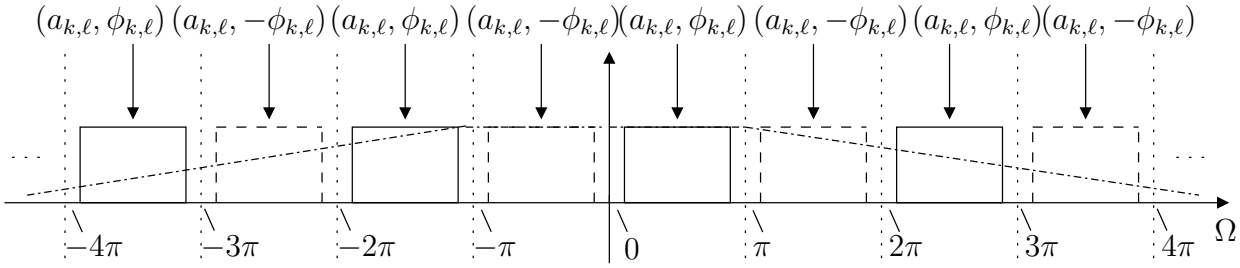

Fig. 2. Graphical illustration of the "useful" and "useless" subcarriers

zero. As a consequence of this fact the continuous output signal $x(t)$ of the OFDM transmitter consists of infinite cosine-shaped signals most of which are heavily attenuated.

As next the output of the OFDM transmitter is further attenuated and phase-rotated by the transmission channel. Because of the fact that the scope of this work is to analyse and demonstrate time-variable effects caused by the OFDM system itself we assume that the transfer function of the channel does not change within one OFDM symbol, a sufficient guard interval is used and that the noise samples all over the transmission path are equal to zero.

At the receiver the continuous time signal is first filtered from the anti-aliasing low-pass analog filter. Afterwards it is passing through the ADC, where it is sampled with the sampling frequency $f_s^{'}$ of the local oscillator, which is generally unequal (very close though) to f_s and once again si-shaped filtered. At this position of the communication path aliasing as well as a frequency shift of the aliased components of the signal and other effects, which will be thoroughly discussed in the next session, occur.

III. Interaction of Aliasing and a Sampling Frequency Offset

As already mentioned main goal of this paragraph is to investigate the effects, which are caused due to the parallel existence of aliasing and a sampling frequency offset. For that reason and in order to provide a distinct analysis we divide it in three main parts. At first the effects caused by aliasing alone are explained and the received power per subcarrier is analytically computed in case of a zero sampling frequency offset by hypothetically applying a IFFT after the FFT at the receiver in order to get the time domain signal (in that way calculations are simplified). In that case the power per subcarrier remains the same before and after the FFT because there are no leakage effects [10]. As second, we assume perfect reconstruction and anti-aliasing filters and discuss the effects originating from the sampling frequency offset. Finally, the effects are combined and formulas, which show that the received power is a periodical function of time, are given.

A. Aliasing

Considering Fig. 1 aliasing is a phenomenon that occurs due to the sampling after the ADC. Actually, aliasing occurs always in real OFDM systems because the amplitude of the

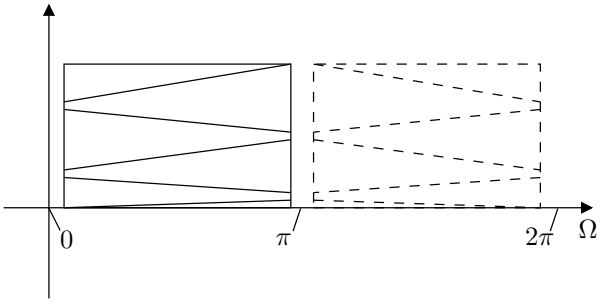

Fig. 3. The effects of aliasing in the interesting (for the FFT) spectrum

infinite - already generated at the transmitter - "useful" and "useless" subcarriers is never ideally attenuated (by the low-pass filters) to zero. Due to the sampling at the receiver the remaining frequency blocks shown in Fig. 2, which are already non-ideally filtered by the reconstruction and the anti-aliasing filter, are again infinitely copied to the corresponding frequencies, which are the original frequencies of the transmitted subcarriers (the "useful" lie between zero and π and the "useless" between π and 2π) shifted by multiples of $\pm 2\pi$. As a consequence of this fact and in respect to the sampling theorem the receiver by using the FFT "looks" to the frequencies between zero and π and reads more power as it was originally transmitted at the subcarrier positions ℓ. This extra power is coming from the aliased subcarriers, which were originally lying in frequency areas, which are the exact subcarrier positions ℓ plus all the infinite multiples of $\pm f_s$. The same happens for the complex conjugated of them (shown in Fig. 3) from π to 2π.

If we now assume a zero sampling frequency offset then no additional effects (e.g. leakage) are caused during the FFT. Because of the fact that it is more convenient to make the calculations shown below in the time domain we assume that we have applied the IFFT to the signal at the output of the FFT again. Because the FFT causes no leakage the output of the hypothetically applied IFFT is the same as the input of the FFT before. If we theoretically separate the time samples of the different subcarriers then we can use $y_{k,\ell}[n]$ shown in Fig. 1 in order to calculate the received power of the signal after the FFT per subcarrier and OFDM symbol, which is in case of aliasing alone the same as the power per subcarrier before the FFT and eventually the deciding value for the system.

Regarding that zero noise samples are assumed we can express the signal after the ADC as follows:

$$y_{k,\ell}[n] = \sum_{i=0}^{+\infty} \alpha_{k,\ell} \, |H(iM+\ell)| \cos(\Omega_\ell n + \phi_{al}(iM+\ell)) + \sum_{i=1}^{+\infty} \alpha_{k,\ell} \, |H(-iM+\ell)| \cos(\Omega_\ell n + \phi_{al}(-iM+\ell)) \,, \tag{3}$$

where $|H(iM+\ell)|$ is the total absolute signal attenuation of the "useful" subcarriers (and all its infinite copies) and given by:

$$\begin{aligned} |H(iM+\ell)| = &|H_{rf}(iM+\ell)| \cdot |H_{af}(iM+\ell)| \cdot |H_c(iM+\ell)| \cdot \\ &\cdot |H_{da}(iM+\ell)| \cdot |H_{ad}(iM+\ell)| \end{aligned} \tag{4}$$

As we already explained in section II the attenuation is caused by the reconstruction and anti-aliasing filters, the channel and the non-ideal ADC and DAC. The total phase rotation ϕ_{al} for the "useful" subcarriers reads:

$$\begin{aligned} \phi_{al}(iM+\ell) = &\phi_{rf}(iM+\ell) + \phi_{af}(iM+\ell) + \phi_c(iM+\ell) \\ &+ \phi_{da}(iM+\ell) + \phi_{ad}(iM+\ell) + \phi_{k,\ell} \\ &= \phi_e(iM+\ell) + \phi_{k,\ell} \,, \end{aligned} \tag{5}$$

where ϕ_e is caused by the filters, the channel, the ADC/DAC and $\phi_{k,\ell}$ by the modulated data.

In respect to Fig. 3 we notice that a part of the aliased subcarriers (the ones which were originally lying in the frequency positions $iM+\ell$) keep their phases and another part (the ones which were originally lying in the frequency positions $iM-\ell$) have to negate their phases. In order to explain this one should consider that the part of the aliased subcarriers that get their phases negatived are the complex conjugated from the "useless" subcarriers and were actually positioned in negative frequencies ($-iM+\ell$). Another way to understand this would be to hypothetically position imaginary half-permeable mirrors at zero, π, 2π etc. and imagine that the mirrors transfer the information from the right to the left from $+\infty$ until zero. That means that these aliased subcarriers inherit the amplitude of the "useless" subcarriers ($|H(-iM+\ell)| = |H(iM-\ell)|$), but get the negative phase:

$$\begin{aligned} \phi_{al}(-iM+\ell) = &\phi_{rf}(-iM+\ell) + \phi_{af}(-iM+\ell) + \phi_c(-iM+\ell) \\ &+ \phi_{da}(-iM+\ell) + \phi_{ad}(-iM+\ell) + \phi_{k,\ell} \\ &= -\phi_{rf}(iM-\ell) - \phi_{af}(iM-\ell) - \phi_c(iM-\ell) \\ &- \phi_{da}(iM-\ell) - \phi_{ad}(iM-\ell) + \phi_{k,\ell} \\ &= -\phi_e(iM-\ell) + \phi_{k,\ell} = -\phi_{al}(iM-\ell) \end{aligned} \tag{6}$$

If we now calculate the received power per symbol and subcarrier we get:

$$\begin{aligned} P'_{k,\ell} &= \frac{1}{M} \sum_{n=0}^{M-1} y^2_{k,\ell}[n] = \frac{1}{M} \sum_{n=0}^{M-1} (\sum_{i=0}^{+\infty} A + \sum_{i=1}^{+\infty} B)^2 \\ &= \frac{1}{M} \sum_{n=0}^{M-1} (\sum_{i=0}^{+\infty} A)^2 + \frac{1}{M} \sum_{n=0}^{M-1} (\sum_{i=1}^{+\infty} B)^2 \\ &+ \frac{2}{M} \sum_{n=0}^{M-1} (\sum_{i=0}^{+\infty} A \cdot \sum_{i=1}^{+\infty} B) \,, \end{aligned} \tag{7}$$

where:

$$A = \alpha_{k,\ell} \cdot |H(iM+\ell)| \cos(\Omega_\ell n + \phi_{al}(iM+\ell))$$

and

$$B = \alpha_{k,\ell} \cdot |H(iM-\ell)| \cos(\Omega_\ell n - \phi_{al}(iM-\ell))$$

It can be shown that for every $\theta, \phi, \rho \in [0, 2\pi]$:

$$\begin{aligned} &2\cos(\theta+\phi) \cdot \cos(\theta+\rho) = \cos(\phi-\rho) \\ &+ \cos(2\theta) \cdot \cos(\phi+\rho) - \sin(2\theta) \cdot \sin(\phi+\rho) \end{aligned} \tag{8}$$

That means that for every $\phi_1, \phi_2 \in [0, 2\pi]$:

$$\sum_{n=0}^{M-1} (2\cos(\Omega_\ell n + \phi_1) \cos(\Omega_\ell n + \phi_2)) = M \cdot \cos(\phi_1 - \phi_2)$$

because:

$$\sum_{n=0}^{M-1} \cos(2\Omega_\ell n) = \sum_{n=0}^{M-1} \sin(2\Omega_\ell n) = 0$$

By using (1) we can calculate the double sums in (7) as shown below:

$$\begin{aligned} \frac{1}{M} \sum_{n=0}^{M-1} (\sum_{i=0}^{+\infty} A)^2 = P_{k,\ell} (&\sum_{i=0}^{+\infty} |H(iM+\ell)|^2 \\ &+ \sum_{j=0}^{+\infty} \sum_{i=0}^{+\infty} |H(jM+\ell)| \cdot |H((i+1)M+\ell)| \\ &\cdot \cos(\phi_{al}(jM+\ell) - \phi_{al}((i+1)M+\ell))) = C \cdot P_{k,\ell} \end{aligned} \tag{9}$$

$$\begin{aligned} \frac{1}{M} \sum_{n=0}^{M-1} (\sum_{i=1}^{+\infty} B)^2 = P_{k,\ell} (&\sum_{i=1}^{+\infty} |H(iM-\ell)|^2 \\ &+ \sum_{j=1}^{+\infty} \sum_{i=1}^{+\infty} |H(jM-\ell)| \cdot |H((i+1)M-\ell)| \\ &\cdot \cos(-\phi_{al}(jM-\ell) + \phi_{al}((i+1)M-\ell))) = D \cdot P_{k,\ell} \end{aligned} \tag{10}$$

$$\begin{aligned} &\frac{2}{M} \sum_{n=0}^{M-1} (\sum_{i=0}^{+\infty} A \cdot \sum_{i=1}^{+\infty} B) = P_{k,\ell} \sum_{j=0}^{+\infty} \sum_{i=1}^{+\infty} |H(jM+\ell)| \cdot \\ &|H(iM-\ell)| \cdot \cos(\phi_{al}(jM+\ell) + \phi_{al}(iM-\ell)) = E \cdot P_{k,\ell} \end{aligned} \tag{11}$$

That means that the power for every subcarrier at the receiver (after the FFT) is directly dependent of the transmitted power at the same frequency as shown below:

$$P_{k,\ell}^{'} = (C + D + E)\, P_{k,\ell} \tag{12}$$

Because the filters' and the channel's attenuation factors and phases are constant with time (that means that C,D and E are also independent of time) the value $\frac{P_{k,\ell}^{'}}{P_{k,\ell}}$ remains also constant with time. Furthermore, it can be shown that the series which are added in C, D and E are converging when using Butterworth or Chebychev low-pass filters. This happens because $|H(iM-\ell)| < 1$ and $|H((i+1)M-\ell)| < |H(iM-\ell)|$. Finally, the larger the filter's order the less the error that is done when a small finite number of "useful" and "useless" subcarriers is used for the calculation of the power at the receiver.

B. Sampling Frequency Offset

In the second step of the analysis we discuss the effects originating from the sampling frequency offset Δf_s alone. For that reason we assume perfect channel conditions as well as perfect initial timing synchronization and low-pass filtering. In this case the sampling frequency at the receiver is slightly different as at the transmitter, which means that the M equidistant subcarrier positions of the FFT at the receiver do not meet the maximum locations of the Dirichlet functions. Indeed, the positioning error grows for larger subcarrier positions and the orthogonality of all the subcarriers is destroyed (ICI occurs). This fact is responsible for the generation of three effects: a) every subcarrier is slightly attenuated (H_{di}) and phase rotated (ϕ_{di}), b) ICI noise is added to every subcarrier and caused by all the other used subcarriers and c) a constantly growing timing offset occurs. The ICI attenuation, which is plotted in Fig. 4 for $M = 128$, depends on the subcarrier index, the FFT-length and the value of the sampling frequency offset and reads:

$$H_{\mathrm{di}}(\ell) = \mathrm{di}_M(\frac{\ell}{M} \cdot \frac{\Delta f_s}{f_s}), \tag{13}$$

where di_M denotes the Dirichlet kernel [11].

As it can be clearly seen in Fig. 4 the Dirichlet attenuation is very small for realistic values of the normalized sampling frequency offset $\frac{\Delta f_s}{f_s}$ e.g. $10-100$ ppm. The same applies for the phase rotation. The second effect of ICI is the noise added to every subcarrier caused by every other subcarrier because the orthogonality is lost. The amplitude of the ICI noise can be written as a sum of noise amplitudes:

$$N_{ici}(f_\ell^{'}) = \alpha_{k,\ell} \sum_{\ell=1,\ell\neq\ell'}^{\frac{M}{2}-1} \mathrm{di}_M(f_\ell^{'} - f_\ell), \tag{14}$$

where $f_\ell^{'} = \ell\frac{f_s^{'}}{M}$ are the new subcarrier frequency positions at the receiver.

The ICI noise power reads:

$$P_{ici}(f_\ell^{'}) = \alpha_{k,\ell}^2 (\sum_{\ell=1,\ell\neq\ell'}^{\frac{M}{2}-1} \mathrm{di}_M(f_\ell^{'} - f_\ell))^2 \tag{15}$$

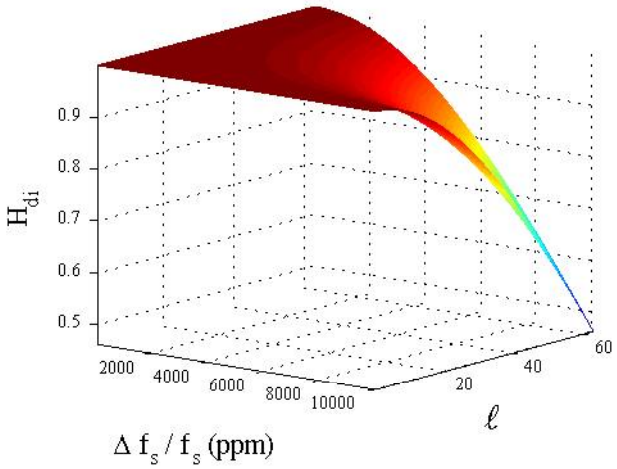

Fig. 4. ICI attenuation due to the sampling frequency offset for M=128

The ICI noise power is a size that is practically neglectable because it is very low for small offsets, so that for 100 ppm the SNR is always larger than 60 dB if no other noise source than ICI exists.

The last effect that is caused by a tolerated sampling frequency offset is a timing offset, which is constantly growing with time if not corrected. Of course, in order to achieve stable OFDM links the timing offset should be always corrected by a correction algorithm. However, there are systems that do not correct the timing offset during the channel and SNR measurement. If so, the phase of every subcarrier is growing with time as shown below:

$$\phi_{\Delta T}(\ell) = 2\pi\ell k(1+\gamma), \tag{16}$$

where $\gamma = \frac{\Delta T_s}{T_s}$ is the normalized sampling period offset and is related to the sampling frequency offset according to:

$$\gamma = \frac{\Delta T_s}{T_s} = (\frac{1}{f_s^{'}} - \frac{1}{f_s})f_s = -\frac{\Delta f_s}{f_s^{'}}, \tag{17}$$

which means that for small values of the normalized sampling frequency offset (e.g. 10-100ppm) γ is approximately its negative.

From (16) it is clear that the phase rotation due to a continuously growing timing offset (caused by the uncorrected sampling frequency offset) is linearly growing with time (here the symbol index k). Also, the larger the frequency position of the subcarrier the larger the increase of the phase rotation. This fact applies, of course, for all the infinite "useful" and "useless" subcarriers and is essential for the explanation of the periodicity of the received power, which is discussed in the following paragraph.

C. Aliasing and a Sampling Frequency Offset

A more realistic approach, where real low-pass filters and non-ideal sampling frequency oscillators are utilized, is analysed in the present subsection. In this case all the effects described in the previous paragraphs are combined in a rather

complicated way. All the "useless" as well as all the "useful" subcarriers at the receiver do not meet the exact frequencies of the transmitter so that the infinite alias subcarriers' frequencies slightly differ from each other. As a consequence after the FFT ICI occurs, where the noise is even larger than in the case described in the previous paragraph because all the aliased subcarriers contribute to the generation of the ICI noise. Furthermore, because of the leakage in the FFT the power of every subcarrier after the FFT is less than its power before it. However, as we already showed the ICI attenuation and phase rotation as well as the ICI noise are so low for realistic values of the frequency offset that they can be practically neglected. As a consequence, we can assume that these effects are minimal and again $y_{k,\ell}[n]$ can be used for the calculation of the power.

In respect to the discussion given at the previous paragraph the effect, which results from the sampling frequency offset itself and should be taken into consideration in the combined case is the constantly growing phase rotation $\phi_{\Delta T}$. That means that the new phase rotation of the infinite "useful" subcarriers and of the complex conjugated "useless" subcarriers, which are used for the calculation of the received power, read:

$$\phi_{al,fo}(iM+\ell) = \phi_{al}(iM+\ell) + \phi_{\Delta T}(iM+\ell) \tag{18}$$

$$\phi_{al,fo}(-iM+\ell) = -\phi_{al}(iM-\ell) + \phi_{\Delta T}(-iM+\ell) \tag{19}$$

So, if one calculates the new received power then the form of (12) remains, but the arguments of the cosines in C, D and E change. The new arguments read:

$$\begin{aligned}\phi_C =&\phi_{al,fo}(jM+\ell) - \phi_{al,fo}((i+1)M+\ell) = \\ &\phi_e(jM+\ell) + \phi_e((i+1)M-\ell) + 2\pi k(j-i-1)M(1+\gamma)\end{aligned} \tag{20}$$

$$\begin{aligned}\phi_D = &\phi_{al,fo}(-jM+\ell) - \phi_{al,fo}(-(i+1)M+\ell) = \\ &-\phi_e(jM-\ell) - \phi_e((i+1)M-\ell) - 2\pi k(j-i-1)M(1+\gamma)\end{aligned} \tag{21}$$

$$\begin{aligned}\phi_E =&\phi_{al,fo}(jM+\ell) - \phi_{al,fo}(-iM+\ell) = \\ &\phi_e(jM+\ell) - \phi_e(iM-\ell) + 2\pi k(j+i)M(1+\gamma)\,,\end{aligned} \tag{22}$$

for the cosines in C, D and E respectively. By combining (12), (9), (10), (11), (20), (21) and (22) we get the final formula that gives the received power for every subcarrier and symbol in case of aliasing and a sampling frequency offset.

Considering the new form of the arguments in the cosines in C, D and E and the forms of C, D and E itself it can be easily derived that the received power is a periodical function of time (here expressed by the OFDM symbol index k). Moreover, the function contains infinite frequencies, the values of which depend on the normalized sampling frequency offset and the FFT-length. Finally, the more the indices i and j in the sums grow the more the amplitudes of these frequencies tend to become zero.

IV. Three Demonstrating Scenarios

In the last section the periodical time-variable effects affecting the received power are demonstrated using the formulas given above. The three following scenarios are examined: a) No reconstruction and no anti-aliasing filter is utilized, b) two 4th order Chebychev filters are used as reconstruction and anti-aliasing filters, c) two 6th order Cauer filters are utilized. Please note that because of the fact that the scope of this work is to analyse phenomena resulting from the OFDM system itself we have normalized the channel's coefficients to 1. Finally, the normalized sampling frequency offset was kept rather small in the value of 10ppm, the chosen FFT-length was 512 and the transmitted power per subcarrier was normalized to 1.

In the first scenario an unrealistic situation, where no low-pass filters are used is shown. This is actually the worst case for the power at the receiver because the amplitudes of the aliased subcarriers are maximized. In section II it was shown that conventional ADC and DAC of type "sample and hold" behave like filters with a characteristic spectrum that has the form of a si function, which is plotted in Fig. 5. It can be easily seen that the ADC/DAC comprise rather bad "filters" because they not only hardly attenuate the frequencies that cause aliasing (from the half of the normalized sampling frequency to $+\infty$) but also insert an attenuation that has a maximum of almost 4dB in the transmission band (from zero to the half of the normalized sampling frequency). Another important observation is that the attenuation is growing slowly so that it is expected that more than the first aliased frequencies (from 0.5 to 1 - the first "useless" subcarriers) are playing an important role in the form of the received power.

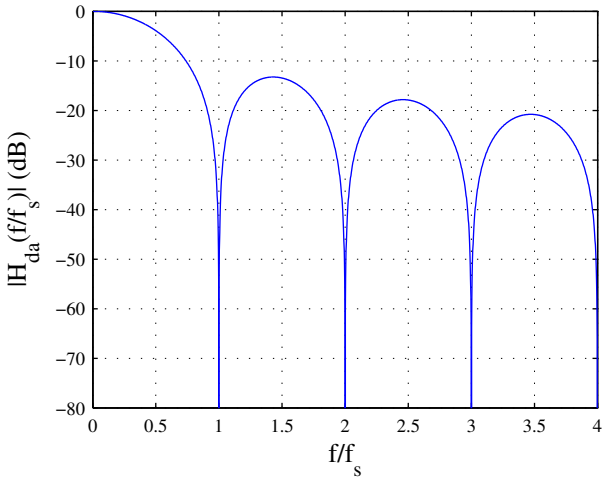

Fig. 5. AD/DA filter's attenuation

Fig. 6 shows the received power at different time points (the OFDM subcarrier index k was changed from 1 to 100) along the frequency in the first scenario. The attenuation of the first "useful" subcarriers as well as the time dependency are clearly observable. The effect is actually so powerful that hardly the first subcarriers could be theoretically utilized for

a data transfer in this case, which would be of course not done because there could be other sources for aliasing than the OFDM system itself so that even the first subcarriers are destroyed. Actually, the worst fact when the received power has the characteristic shown in Fig. 6 is not the attenuation of the utilized subcarriers but the time-variability and the large jumps in the values of the received power that is destroying the SNR. Please note that during the simulations we have sequentially used a growing number of aliased subcarriers starting with the first "useless" (from 0.5 to 1) and the second "useful" (from 1 to 1.5) ones. Thereby we noticed that after the third period (from 2.5 to 3.5) no remarkable impact was seen in the generated figures. It was furthermore observed that changes in the normalised frequency sampling offset didn't affect the form of the 2-D plot but only the period of the power's fluctuation, which is clear due to the form of (20), (21) and (22). This fact can be easily seen by the corresponding 3-D plots (simulations done for different values of γ), where the third dimension is the time and which are not shown for reasons of redundancy.

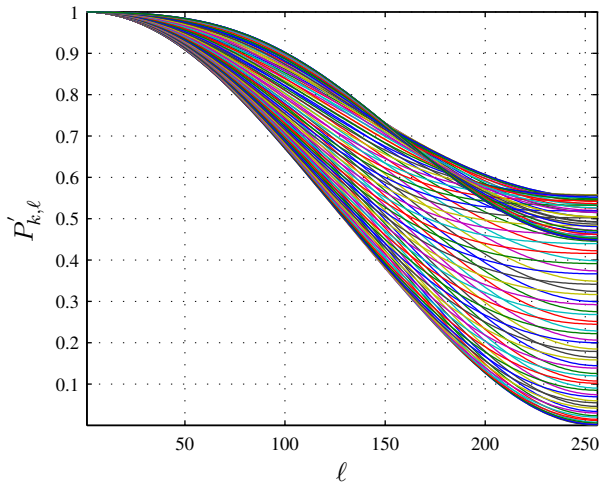

Fig. 6. Received power in the first scenario

In the second scenario we investigate the case, where two 4th order Chebychev filters are utilized (attenuation plotted in Fig. 7 - ripple equal to 0.125dB). This is a realistic scenario, where most of the aliased subcarriers are sufficiently filtered and the filters are relatively easy to implement. Fig. 8 shows the received power per subcarrier in that case. The first "useful" subcarriers are again attenuated by the ADC and the DAC and more than 50 subcarriers are severely affected by the effects. In order to demonstrate how large the power's fluctuation is we assumed that the ADC and DAC are perfect (attenuation caused equals zero), which is even more realistic because the reconstruction and anti-aliasing filters are normally designed in a way that the attenuation caused by the ADC and the DAC is almost eliminated. The results are plotted in Fig. 9. The received power fluctuates in a way that even more power (coming from the aliased subcarriers) than given at the specific frequencies is received according to the OFDM symbol index. During the simulations we observed that for the specific filters only the first "useless" subcarriers caused noticeable aliasing effects.

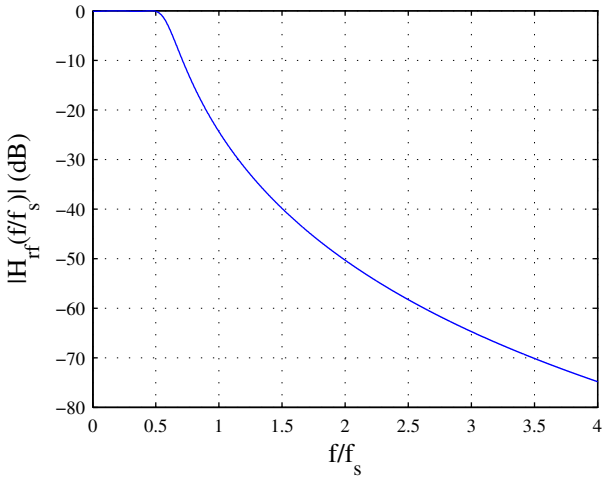

Fig. 7. Anti-aliasing/reconstruction filter's attenuation - Chebychev 4th order

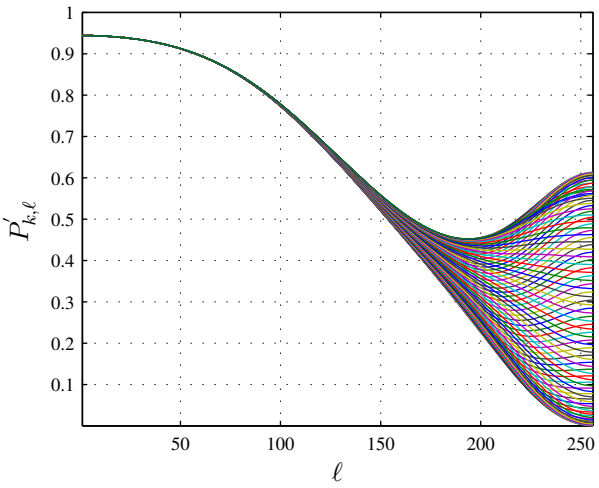

Fig. 8. Received power in the second scenario

In the last scenario two 6th order elliptic (Cauer) filters were used. This is a more optimistic case because the filters are more complicated to implement. From the form of the received power (see Fig. 11, Fig. 12) it is clear that this is the best scenario as the received power remains rather constant in time for the most subcarriers. However, even in this case there are subcarriers near the Nyquist frequency, which are heavily affected and improper for data transfer. This happens because the filters are not steep enough to provide enough attenuation near the Nyquist frequency so that the impact of the first aliased subcarriers is still quite noticeable.

Generally, the fluctuations in the received power grow with the subcarrier index. Actually, the 2-D form of these changes resembles a bouquet of flowers ("Blumenstrauss" in German), which is rotated 90° (see Fig. 8, 9, 11 and 12). This is rather

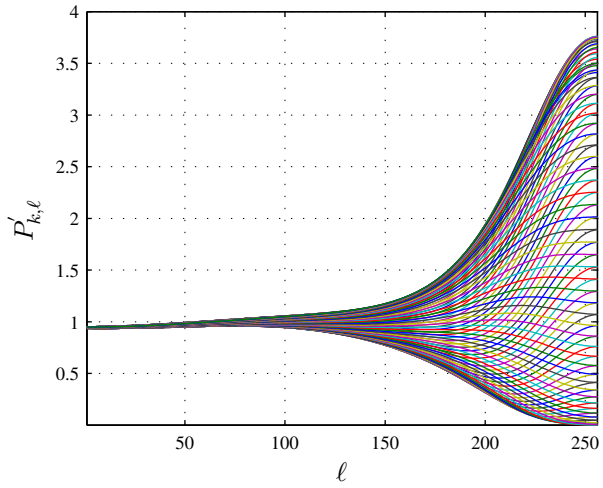

Fig. 9. Received power in the second scenario (perfect AD/DA assumed)

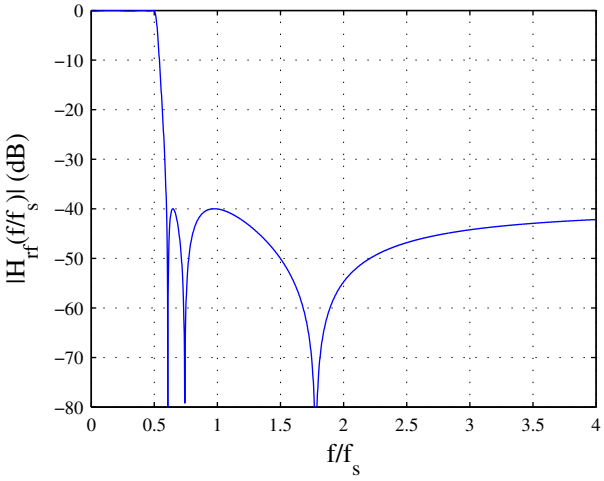

Fig. 10. Anti-aliasing/reconstruction filter's attenuation - Cauer 6th order

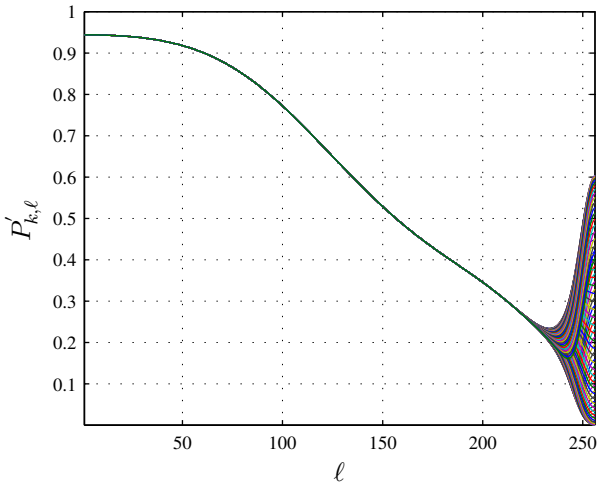

Fig. 11. Received power in the third scenario

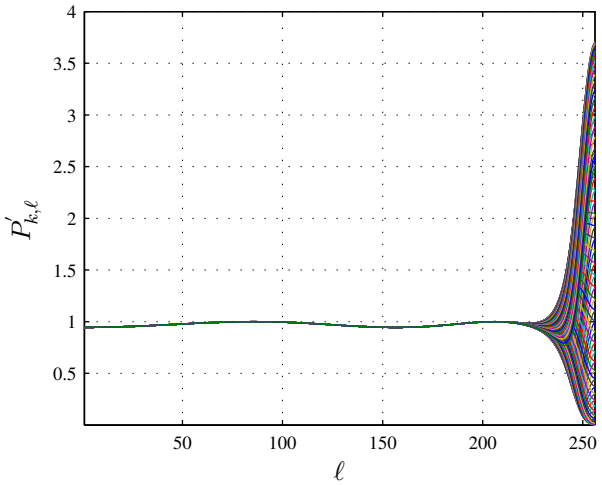

Fig. 12. Received power in the third scenario (perfect AD/DA assumed)

expected because the least filtered frequencies, where the first aliased subcarriers lie, are mirrored in the frequency area between zero and π (see Fig. 3) so that the highest frequencies (close to the Nyquist frequency) are mostly affected. The length of the "stick" of the bouquet as well as the thickness of the "flowers" in the bouquet increases with the abruptness of the low-pass filter (e.g. compare between Fig. 9 and Fig. 12)).

From the results shown in this section it is also clear that most of the theoretically infinite aliased subcarriers play practically no role in the changes of the received power in time. The filtering threshold lies approximately by -25dB, which means that if normal low-pass filters are utilized, only the subcarriers lying between π and 2π can be used to predict the form of the received power and decide whether the filter is good enough or if some subcarriers should be left out of the transmission scheme. Indeed, the exception of at least one subcarrier (the next one near the Nyquist frequency) seems to be unavoidable if the OFDM system is designed in the way we have described in this work. The number of these subcarriers is yet dependent on the FFT-length (the larger M is the narrower the available transition bandwidth for the low-pass filters is for a given sampling frequency) and the filter's characteristic. That is why these system parameters should by carefully chosen in respect to the given analysis and the system's specifications.

V. Conclusions

In this work the effects caused by the combination of two well-known drawbacks of OFDM systems, namely aliasing and a sampling frequency offset, were analysed. It lies in the nature of OFDM that even small sampling frequency offsets cause large phase rotations to the utilized subcarriers, which depend on the subcarrier's frequency and the symbol index. The parallel existence of aliasing yet results in a combined effect, where the aliased subcarriers, which are heavily phase rotated as they lie in large frequencies, are added to their corresponding subcarriers, which lie between zero and the Nyquist frequency and are therefore less phase rotated. The result of these theoretically infinite additions is a large fluctuation of

the received power, which grows with the subcarrier's index, the FFT-length and the inverse of the attenuation factors of the utilized low-pass filters. Due to the power fluctuations, which can be exactly calculated using the given formulas, there are severe degradations in the SNR, which can eventually lead to the exclusion of some subcarriers from the transmission scheme.

REFERENCES

[1] R. S. A.V. Oppenheim and J. Buck, "Discrete-time signal processing (2nd edition)," Feb 1999.

[2] M. V. B. T. Pollet and M. Moeneclaey, "Ber sensitivity of ofdm systems to carrier frequency offset and wiener phase noise," *IEEE Transactions on Communications*, vol. 43, no. 234, pp. 191–193, Feb-Mar-Apr 1995.

[3] Y. Li and L. Cimini, "Bounds on the interchannel interference of ofdm in time-varying impairments," *IEEE Transactions on Communications*, vol. 49, no. 3, pp. 401–404, March 2001.

[4] S.-G. H. Y. Zhao, "Sensitivity to doppler shift and carrier frequency errors in ofdm systems-the consequences and solutions," *IEEE 46th Vehicular Technology Conference, 1996. 'Mobile Technology for the Human Race'*, vol. 3, pp. 1564–1568, April 1996.

[5] M. Sliskovic, "Sampling frequency offset estimation and correction in OFDM systems," *The 8th IEEE International Conference on Electronics, Circuits and Systems, 2001. ICECS 2001*, vol. 1, pp. 437 – 440, Sept. 2001.

[6] J. Armstrong, "Analysis of new and existing methods of reducing intercarrier interference due to carrier frequency offset in ofdm," *IEEE Transactions on Communications*, vol. 47, no. 3, pp. 365–369, March 1999.

[7] L. Wang and C. Tellambura, "A novel ici cancellation technique for ofdm systems using adaptive mapping signal constellation," *PACRIM. 2003 IEEE Pacific Rim Conference on Communications, Computers and signal Processing, 2003*, vol. 1, pp. 442–445, Aug 2003.

[8] S. X. C. Jun, J.W. Mark, "Ici cancellation in ofdm wireless communication systems," *GLOBECOM '02 IEEE Global Telecommunications Conference, 2002*, vol. 1, pp. 656–660, Nov 2002.

[9] S.-G. H. Y. Zhao, "Intercarrier interference self-cancellation scheme for ofdm mobile communication systems," *IEEE Transactions on Communications*, vol. 49, no. 7, pp. 1185–1191, July 2001.

[10] J. Schwarz, "Enhancing the Spectral Selectivity of Discrete Multi-Tone Modulation," Dissertation, Universität Mannheim, 2006.

[11] K. D. Kammeyer and K. Kroschel, *Digitale Signalverarbeitung*, 5th ed. Stuttgart: B. G. Teubner, 2002.

Ilias Trachanas was born in Athens, Greece, in 1982. He received the Diploma in electrical engineering from the National Technical University of Athens, Athens, Greece, in 2004. Since 2004 he is with the University of Mannheim, Mannheim, Germany, as a research and teaching assistant.

He is currently working on a project about IP communications over the medium voltage network funded by a major European electrical power company. He serves as reviewer for the IEEE Transactions on Wireless Communications and is a member of VDE (Germany). His research interests include digital signal processing, OFDM, synchronization, channel characterization and modeling, detection and estimation, interference rejection and their application to powerline and wireless telecommunications.

Norbert J. Fliege (M'89, SM'90) received the diplom degree (Dipl.-Ing.) and the doctor degree (Dr.-Ing.) in 1971, both from the University of Karlsruhe, Germany.

Since 1978, he was an associate professor at the same university. In 1980, he was a visiting professor at ESIEE in Paris. From 1982 to 1996, he was a Full Professor and Head of the Telecommunication Institute at Hamburg University of Technology in Hamburg, Germany. Since 1996, he has been a Full Professor of Electrical Engineering and Computer Technology at University of Mannheim, Germany. Since 1968, Dr. Fliege has been engaged in research work on fields like active filters, digital filters, communication circuits and software, digital audio, and multirate digital signal processing. In addition, he served as a Department Chairman and as Head of a research center. He has also founded a company providing telecommunication equipment.

Dr. Fliege has published more than hundred papers, most of them in international magazines and conference proceedings, and four books, one of them with the title "Multirate Digital Signal Processing", published by John Wiley and Sons in 1994. Dr. Fliege is a Senior Member IEEE, a member of EURASIP, and a member of VDE (Germany). He has received several national and international awards. In 1997, he has got the honorary doctorate from University of Rostock, Germany. In 2000, he was awarded an IEEE Fellow for contributions to analog and digital signal processing, and to engineering education.